Published in final edited form as:
Pflugers Arch. 2007 November ; 455(2): 333–348. doi:10.1007/s00424-007-0282-7.

The selectivity, voltage-dependence and acid sensitivity of the tandem pore potassium channel TASK-1: contributions of the pore domains

KH Yuill[1,4,*], **PJ Stansfeld**[2,*], **I Ashmole**[1,*], **MJ Sutcliffe**[3], and **PR Stanfield**[1,†]

[1]Molecular Physiology Group, Department of Biological Sciences, University of Warwick, Coventry CV4 7AL, UK

[2]Department of Cell Physiology and Pharmacology, University of Leicester, PO Box 138, Leicester, LE1 9HN, UK

[3]Manchester Interdisciplinary Biocentre, University of Manchester, 131 Princess Street, Manchester, M1 7DN, UK

[4]Department of Pharmacy and Pharmacology, University of Bath, Bath BA2 7AY, UK

Abstract

We have investigated the contribution to ionic selectivity of residues in the selectivity filter and pore helices of the P1 and P2 domains in the acid sensitive potassium channel TASK-1. We used site directed mutagenesis and electrophysiological studies, assisted by structural models built through computational methods. We have measured selectivity in channels expressed in *Xenopus* oocytes, using voltage clamp to measure shifts in reversal potential and current amplitudes when Rb^+ or Na^+ replaced extracellular K^+. Both P1 and P2 contribute to selectivity and most mutations, including mutation of residues in the triplets GYG and GFG in P1 and P2, made channels non-selective. We interpret the effects of these – and of other mutations – in terms of the way the pore is likely to be stabilised structurally. We show also that residues in the outer pore mouth contribute to selectivity in TASK-1. Mutations resulting in loss of selectivity (*e.g.* I94S, G95A) were associated with slowing of the response of channels to depolarisation. More important physiologically, pH sensitivity is also lost or altered by such mutations. Mutations that retained selectivity (*e.g.* I94L, I94V) also retained their response to acidification. It is likely that responses both to voltage and pH changes involve gating at the selectivity filter.

Keywords

potassium channel; ionic selectivity; pH sensitivity; voltage dependence

INTRODUCTION

Sequencing and functional studies have uncovered a great diversity among potassium ion channels, with several gene families now established. Members of the tandem pore (K_{2P}) or *KCNK* family [29, 18, 41] contribute to the setting of resting potentials of a wide variety of cells, a function they may share with members of other ion channel families, including members of the inward rectifier or Kir family [49] and of the CLC family [21]. While

[†]Corresponding author: PR Stanfield Molecular Physiology Group Department of Biological Sciences University of Warwick Coventry CV4 7AL Telephone (+44) 2476 572 503 FAX (+44) 2476 523 568 E mail: p.r.stanfield@warwick.ac.uk.
[*]These authors contributed equally to this paper.

Europe PMC Funders Author Manuscripts

tandem pore channels are often described as leakage channels, it is known that they do not act simply as open conduits for the flux of K^+ across the membrane. Single channel recording shows that channels spend time shut in physiological conditions, so that open state probability (P_{open}) may be very much less than unity (*e.g.* ref [26]). Further, many physiological factors modulate channel activity, altering P_{open}. These factors include pH, protein phosphorylation, arachidonic acid, membrane stretch, inositol phospholipids, Ca^{2+}, and temperature [18, 41, 11, 12]. In addition, tandem pore channels either are [32, 56] – or may under certain circumstances [5, 37] be – gated by voltage.

In the tandem pore (*KCNK*) family, channel subunits each possess two pore (P-) regions in tandem. The primary structure of these two pore regions is not identical and, though both regions are likely to contribute to ionic selectivity, the contributions of the two differ in subtle ways (see *e.g.* ref [7]). Classically, the P-region of K^+ channels contains the consensus sequence `TxxTxGYG`, but this consensus does not hold firmly in the tandem pore family. The peptide bonds between the last five residues of this sequence contribute a series of rings of carbonyl oxygen atoms through which K^+ ions move (*e.g.* ref [15]). Set at the correct distance, these form binding sites for K^+. The side chain hydroxyl of the second Thr residue of the motif also contributes to the innermost binding site. This mechanism of selectivity, first proposed by Bezanilla & Armstrong (ref [3]), with carbonyl oxygens acting as surrogates for the oxygens of water in solution, is now universally accepted following the solution of the structure of the bacterial K^+ channel KcsA by X-ray crystallography [15]. In this paper we investigate the effects of altering residues in the pore regions of the P1 and P2 domains on ionic selectivity of TASK-1.

TASK-1 is important physiologically since it is sensitive to changes of extracellular pH and is shut in acid conditions [16, 24, 28]. Regulation by extracellular pH has suggested roles in the maintenance of acid-base balance, for example in the regulation of respiration by central [2] and peripheral chemoreceptors [6]. The sensitivity to a change of extracellular pH is thought to be endowed by a His residue (H98) in the first (P1) of two tandem pore regions [26, 44, 1, 33, 38]. This residue lies at the outer mouth of the pore, at a position occupied by aspartate in P2 of TASK-1 and in the single pore region of many members of other K^+ channel families. However, the abolition of pH sensitivity in H98N, for example, is not complete in TASK-1, and other residues may well contribute to acid sensing [1, 38]. These channels also show voltage-dependence, consistent with an increased open probability under depolarisation [32]. Both voltage dependence and pH sensitivity of TASK-1 are affected by extracellular [K^+] [32]. We have therefore considered, in making mutations of the pore region, whether the responses of TASK-1 to depolarisation and to acidification belong to the class of gating thought to occur at the selectivity filter (see *e.g.* refs [4, 54]).

We show that changes in the structure of the pore alter ionic selectivity, as anticipated, and we consider our findings in terms of a structural model of TASK-1. Changes in the structure of the pore do indeed also alter the response both to membrane potential and to acidification. Mutations of the selectivity sequence that abolish selectivity appear to slow the response to depolarisation and reduce acid sensitivity. We consider that these responses are likely to involve a change in the conformation of the selectivity filter.

METHODS

Molecular biology

Experiments used murine TASK-1, cloned from mouse total brain RNA [55]. In a few experiments, we used a concatameric dimer of TASK-1, whose construction has also been described previously [55]. Mutants were generated by the QuikChange method (Stratagene) and all mutations were verified by sequencing the entire mutant cDNA, using the molecular

biology service in the Department of Biological Sciences, University of Warwick. We found TASK-1 expression difficult to achieve routinely in HEK293 or CHO cells and accordingly used expression in *Xenopus* oocytes. cRNAs were synthesised *in vitro* from *Mlu*I-linearised pBF vector, using SP6 polymerase (Ambion).

Electrophysiology

Electrophysiological recordings were carried out on TASK-1 channels expressed in oocytes obtained from *Xenopus* frogs anaesthetised by immersion in 0.3% (w/v) MS222 and killed by destruction of the brain and spinal cord. Oocytes were injected with up to 50ng cRNA and recordings were made 1 – 5 days after injection.

We used a GeneClamp 500B amplifier, a Digidata 1322A interface and pClamp version 8.2 software (all Axon Instruments, Foster City, CA) to measure ionic currents under two-electrode voltage clamp. Impaling borosilicate glass microelectrodes were used backfilled with 3M KCl. Currents were filtered at 2kHz and digitised at 10kHz. Analysis also used pClamp software and curve fitting used this software or Sigmaplot 2001 or version 9.0.

Experiments were carried out at room temperature (~20°C) using extracellular solutions containing permeant cations at 70mM. The K^+ solution contained (mmol.l^{-1}): 70 KCl, 26 *N*-methyl-D-glucamine, 1 $CaCl_2$, 1 $MgCl_2$, 10 HEPES, pH adjusted using HCl. In some experiments, we omitted $CaCl_2$ and $MgCl_2$ from our experimental solutions to test whether voltage dependence was generated by reversal of voltage dependent blockage by divalent cations or whether currents activated by Ca^{2+} entry materially affected our results.

In experiments to measure ionic selectivity against Rb^+ and Na^+, we replaced KCl in the experimental (extracellular) solution by RbCl or NaCl. As is conventional, permeability ratios (P_X/P_K) were measured from the shift in reversal potential (ΔE_{rev}) occurring when Rb^+ or Na^+ replaced K^+ in the extracellular solution, that is from

$$\Delta E_{rev} = \frac{RT}{F}.\ln\frac{P_X[X^+]_o}{P_K[K^+]_o} \quad (1)$$

where X^+ represents either Rb^+ or K^+. The experiments were carried out at pH 7.8 to maximise pH-sensitive currents so far as possible. Since small endogenous currents are found in oocytes, the values given for P_{Na}/P_K (*e.g.* for wild type) correspond to an upper limit.

To test pH-sensitivity, we used 10mM HEPES (pH adjusted using HCl) for solutions at pH 7.0 to 8.5, PIPES for pH_o 6.5, and MES for pH_o 6.0. To analyse, we fitted the responses to ΔpH_o using an expression which assumes reduction in current is proportional to the fractional protonation of a regulating site:

$$y = a.\left\{1+\frac{[H^+]_o}{K_a}\right\}^{-1} + b \quad (2)$$

Here, y is the current, normalised to its value at pH_o 8.5, and K_a is the equilibrium constant (we give the pK_a in the text of this paper). $a/(a + b)$ is the fraction of the current that is sensitive to acidification, with $b/(a + b)$ the fractional current remaining at low pH_o. We set b to zero if its fitted value was less than 0.05 (as in wild type channels).

We made statistical comparison of experimental results from mutants with those from wild type using ANOVA with a Dunnett multiple comparisons test. The results of this comparison are given in Tables 1 & 2. Comparison among mutants used a Tukey-Kramer

multiple comparisons test. Additional results detailing the relative permeabilities (Supplementary Table 1) and pH sensitivities (Supplementary Table 2) are given in supplementary material.

Sequence analysis and homology modelling

The secondary structure and transmembrane topology for murine TASK-1 (Swissprot accession code 035111) were predicted using the PSI-Prediction server [36]. Homology modelling was used to predict structures of the transmembrane domains. KcsA was chosen as the primary structural template for TASK-1 (Protein Data Bank (PDB) accession code 1K4C [57]). We used ClustalX to align two copies of the sequence of KcsA – modified to resemble a dimer by merging two copies of the monomer – with the sequence of the dimeric murine TASK-1 (supplementary Fig. 1).

The homology models of TASK-1 were created using Modeller 6v2 [46]. For each set of ten TASK-1 models generated, the lowest energy model was selected. Initial structures of TASK-1 were based on KcsA, though these models were modified to incorporate the M2-M3 linker and the linker between M1 and P1, which is also known as the self-interacting domain (SID) [29, 30]. The orientation by which M2 is connected to M3 may only be hypothesised. Based on the distances between the outer and inner helices of the K^+ channel crystal structures, including KcsA (PDB accession code: 1K4C), KirBac1.1 (1P7B) and KvAP (1ORQ), the minimum M2-M3 separation was obtained in a clockwise rotation, as viewed from above. The orientation and secondary structure of the M2-M3 linker therefore shares equivalence with the slide helix of KirBac1.1. To incorporate the M2-M3 linker, the KirBac1.1 structure (1P7B) was aligned with the structure of KcsA, with KirBac1.1 used to model both the M2-M3 linker and M3 helix.

The self-interacting domain was modelled based on an equivalent region of the crystal structure of the alkyl hydroperoxide reductase subunit F (AHPF; 1HYU) [53], which shares sequence and secondary structural similarity. The domain was connected to the top of the channel based on four restraints: (i) The N-terminus of the first helix of the linker was positioned in close proximity to the C-terminus of the M1 helix, since they are separated by at most three residues; (ii) the second helix was angled so that its C-terminal end was not too far from the N-terminal end of the P1 pore helix; (iii) N53 was mutated to Cys and a disulphide bridge was modelled between the substituted Cys residues; and (iv) secondary structure restraints were imposed to retain the two predicted helices. Once the initial model was created, the Cys residues were mutated back to Asn.

The extended loop between the selectivity filter of P2 and M4 is eight residues longer in TASK-1 than in KcsA and thus this was modelled by using the webserver LOBO (Loop Build-up and Optimization) [52]. The first of the eight solutions generated was chosen as it agreed most closely with the secondary structure prediction. There are no templates with structural equivalence for the C-terminal region of the TASK-1 sequence and thus this region was omitted from the models. The positions of ions and water molecules were modelled from the KcsA structure. The mutants of TASK-1 were modelled and analysed using the molecular graphics program Pymol [14].

RESULTS

Evaluation of the TASK-1 comparative model

A structural model of TASK-1 has been constructed of the region from Met1, at the N-terminus, through to Arg257, in the M4 transmembrane helix. In addition to describing the pore domain of the TASK-1 channel, which is already relatively well represented by analogy with the available K^+ channel crystal structures, the model hypothesises for the first

Europe PMC Funders Author Manuscripts

time the structure of the domain that links the M1 transmembrane helix to the pore helix in the P1 segment, and provides a picture of the α-helical structure and orientation of the M2-M3 linker that connects the P1 and P2 segments. The structure is shown schematically in supplementary Fig. 1B. The differences in the structures of the P1 and P2 segments of the TASK-1 model are shown in Fig. 1. The structure is in its closed conformation, but serves to illustrate the residues contributing the pore regions, which are the subject of this study.

The residues in the region comprising the pore helix through to the inner transmembrane helix share a 40 % similarity in P1 and 37 % in P2 with the template structure, KcsA. In addition, among the residues in and around the selectivity filter, those that were mutated in this study share a 67 % similarity in P1 and 50 % in P2. This level of homology is high enough to create a relatively accurate model of the TASK-1 channel, which is stable in subsequent molecular dynamics simulations. There are several differences between the sequences of the P-regions of P1 (Fig. 1C) and P2 (Fig. 1D). These differences are accentuated structurally with the aromatic of the `G(Y/F)G` motif and are reflected in the residues surrounding the filter, making the region behind the selectivity filter of P1 relatively more hydrophilic than that behind the selectivity filter of P2. In the region of interest, a 58 % sequence identity is shared between the P1 and P2 segments of TASK-1.

Permeability of TASK-1 to Rb^+ and Na^+

Fig. 2 shows records and current-voltage relationships for wild type TASK-1 in the presence of 70mM $[K^+]_o$, $[Rb^+]_o$, and $[Na^+]_o$. As described previously [16, 28], current-voltage relations show weak outward rectification in K^+ solutions. This rectification is close to, but not identical with, that expected from constant field theory, with a higher concentration of K^+ internally. Outward currents are larger than expected from these considerations (Fig. 2C), since channels show a weakly voltage dependent gating (see below), which occurs over a wide range of voltages [32].

As we have previously shown [55], Rb^+ readily permeates wild type TASK-1 channels, relative permeability being measured using Eqn (1). Under hyperpolarisation, Rb^+ currents are however smaller than K^+ currents, and Rb^+ in the external solution impedes K^+ efflux at depolarising voltages up to +80mV (Fig. 2B, C), suggesting that Rb^+ acts as a blocking cation (see also ref [39]). As previously described by ourselves [55] and others [32], the relative permeability to Na^+ is low (Table 1; Fig. 2D); as is the case for other K^+ channels, Na^+ may be considered essentially impermeant.

Mutations of the pore regions – mutations of the selectivity filter in P1 and P2

We have made mutations of many residues of the selectivity filter and pore helix (which helps stabilise the selectivity filter) of both the P1 and P2 domains of TASK-1. The effect of these mutations on the relative permeabilities of K^+, Rb^+ and Na^+ is documented in Table 1.

GYG and GFG triplets: replacement of glycines

Mutations of the triplet of residues `GYG` in P1 and `GFG` in P2 all alter selectivity (Table 1: Fig. 3). It was anticipated that replacement of Gly residues would abolish selectivity and this is indeed the result found. Channels where either G95 or G97 is replaced by Ala fail to distinguish K^+ from Rb^+ or Na^+ (Table 1 and Fig. 3). Similar results were obtained by replacing the equivalent residues in P2, G201 and 203, in turn by Ala (Table 1).

Table 1 also gives the results of replacement of G95 by glutamate or aspartate. Others have already identified G95E as a loss of function mutation [22, 27, 42], acting as a dominant negative when co-expressed with other TASK subunits. The mutation is found in TASK-5 of some humans, owing to single nucleotide polymorphism at this point in the sequence [22,

25]. We were unable to measure currents in oocytes injected with the cRNA of G95E or of a concatameric dimer (G95E/WT) where only one subunit of the dimeric structure has the mutation.

However the mutant G95D produced functional, non-selective channels (Table 1), as did the concatameric channel G95D/WT. There was no significant difference between G95D and the G95D/WT concatamer in the quantities used to measure selectivity (Table 1; $P>0.05$ in all cases). The replacement of a single Gly95 by Asp in the concatameric dimer appears as damaging to selectivity as is replacement of the residue in both subunits.

GYG and GFG triplets: replacement of aromatic residues

The effects of alterations of the central residue of the GYG or GFG triplet are more striking in TASK-1 than in Kv or in Kir, since even conservative substitutions abolish selectivity. Among the residues we used to replace Y96, only Phe produced functional channels and we were unable to measure currents when Y96 was substituted by Leu, Met or Val. Y96F channels were non-selective (Table 1; Fig. 4A, B). While the effects of the substitution of Y96 by F are less substantial than those caused by replacement of G95 and G97, the loss of selectivity is much greater than that seen in either *Shaker* Kv channels or in Kir [20, 47].

However, it was possible to replace F202 with one of a number of alternatives (Table 1). All replacements affected selectivity including F202Y (Table 1, Fig. 4C, D). This result contrasts with that of Hajdú *et al.* (ref [19]), who argued for retention of selectivity with the change F to Y. In fact, in our experiments, mutants F202A and F202V were, alongside G95A, the least selective of any mutants we have made (Table 1). These differences between P1 and P2 and between TASK-1 and other K^+ channels are likely to reflect different residues stabilising the selectivity filter.

In our model (Fig. 4E, F), Y96 is predicted to point into an environment that is more hydrophilic than that seen by F202 at the back of P2. The model predicts that Y96 can form hydrogen bonds with T196 in the P2 pore helix and S224 in M4, and that other hydrophilic residues, including Y85, T89, and Y192, may contribute to the hydrogen bonding network surrounding Y96. In terms of the model, reduced selectivity is explained in terms of the loss of these bonds in Y96F and the resultant destabilising of the pore structure. Our model does not show the contact between Y96 and D204 that others have suggested [7]. F202 is predicted to lie in a more hydrophobic environment, with nearby residues including F86 and V90 in the pore helix of P1 and I195 in the pore helix of P2. However, in F202Y hydrogen bonding may occur with Y191 in the pore helix of P2, the lack of selectivity being associated with the altered structure.

GY(F)G and effects of mutation on voltage dependent gating

Fig. 5A shows that wild type currents increase with time under depolarisation. The process was little affected by omission of both Ca^{2+} and Mg^{2+} from our experimental (extracellular) solutions (data not shown), and is then not due to ionic blockage of channels by these divalent cations. Lopes *et al.* [32] have already described this gating process and shown it to be dependent on the concentration of K^+ in the extracellular solution and more prominent in physiological $[K^+]_o$. The observation that, at a given voltage, channels are more likely to be shut in low $[K^+]_o$ raises the possibility that voltage gating is associated with conformation changes in the filter.

Consistent with such a hypothesis, mutations of the selectivity filter resulted in a change in the kinetics of the response to voltage, and this alteration is illustrated in Fig. 5. The mutant G95A shows a significant slowing of the increase in current under depolarisation. Fig. 5A

shows current records for wild type and G95A. These and currents through other mutant channels were fit with a function

$$I_K(t) = A_1.\exp(-t/\tau_1) + A_2.\exp(-t/\tau_2) + C \quad (3)$$

with two exponential arguments, with fast and slow components (see also Fig. 5B). Depolarisation results in an instantaneous step in current, which then increases over several 100ms. In wild type at +100mV, this increase in current represents 0.23 ± 0.02 (n = 16) of the steady state current. In G95A, the fraction is increased significantly ($P < 0.01$) to 0.41 ± 0.03 (n = 9).

The time constants for this increase in current are illustrated in Fig. 5C. Lopes *et al.*. (ref [32]) have shown that these time constants are only weakly dependent on voltage, describing those for activation as changing e-fold per 250mV, those for deactivation e-fold per 500mV. This weak voltage dependence makes full analysis of the gating process difficult and we have not attempted for the present to quantify the gating charge. However the time constants for activation are increased significantly in G95A over their values in wild type. Further the slow component of activation is increased in this mutant. In G95A, it represents 0.30 ± 0.03 of the steady state current, while in wild type it represents only 0.11 ± 0.02 of steady state current, a difference that is significant ($P < 0.01$; n = 8). Similar results were found with other mutants of the GY(F)G triplet. The mutant G95D, which introduces a charged residue into P1 and might be expected to introduce an altered response to voltage, did not produce results different from those with G95A (data not shown).

Response to acidification of mutants of GY(F)G

TASK-1 is sensitive to extracellular acidification and several authors have described the pH-sensitivity of wild type TASK-1 channels and its weak voltage dependence [16, 32, 1, 38]. Fitting Eqn 2 to the relationship between wild type current and pH_o gave values for pK_a of 6.66 ± 0.05 and 6.57 ± 0.06 (13) at membrane potentials of −40 and +40mV respectively (Fig. 6A, B). Several authors have described how mutation of H98 at the mouth of the pore reduced acid sensitivity [26, 44, 1, 33, 38].

However, as Fig. 6A, B shows, currents through the mutant G95A were also little altered by acidification. In this mutant, currents at pH 6 and +40mV were still 0.85 ± 0.05 of their amplitude at pH 8.5 indicating that little inhibition occurred. In wild type at pH 6, currents were 0.24 ± 0.01 (12) of their amplitude at pH 8.5 (Fig. 6A).

Replacement of Tyr96 by Phe also alters pH sensitivity. In this instance (Fig. 6C), considerable K^+ current persists at low pH_o, but currents increase under alkalinisation. We have previously described a similar response for D204H and D204N mutant channels [55]. Mutation of Y96 (and D204) thus results in channels that are insensitive to pH changes around physiological pH but are further activated upon alkalinisation, a property reminiscent of, but not identical with, the response of alkali-sensitive tandem-pore channels such as TASK-2 and other members of the TALK subfamily [45, 13, 17]. Chapman *et al.* [7] have proposed an interaction between residues Y96 and D204 in TASK-1, and a similarity in response of these mutants to acidification (Y96F here, D204N in ref [55]) might be taken as further evidence for such an interaction. However other mutants have similar properties. The mutant G97A responds to ΔpH_o in a similar way to that shown by Y96F (Table 2), its properties contrasting with those of G95A and I94S, T (see below), where the response to acidification is effectively abolished. The mutant F202Y shows little reduction in current in acid conditions (Table 2; Fig. 6D).

Thus, mutants of the selectivity filter have radically altered responses to changes of extracellular pH (ΔpH_o). The simplest explanation is that the response to acidification involves gating at the pore and that disrupting the pore structure disrupts these gating movements.

Isoleucine 94 and 200: effects on ionic selectivity—We now test further the hypotheses that both voltage dependence and pH sensitivity involve the selectivity filter using mutants of I94 and I200 (equivalent residues in the P1 and P2 domains, respectively; Fig. 1). In Kv [51] and Kir channels [40] effects on selectivity of the mutation of the equivalent residue were correlated with the hydrophobicity of the side chain of the substituted residue. A similar correlation was found in TASK-1 (Table 1; Fig. 7) and we describe first the ionic selectivity of these mutants.

We found that replacement of I94 (P1) with the hydrophobic residues Leu and Val had relatively little effect on selectivity against Na^+ in particular (Table 1, Fig. 7). But replacement by the hydrophilic residues Ser or Thr made channels non-selective (Table 1; Fig. 7C, D). The loss of selectivity against Na^+ was the more complete in I94S perhaps because the bulkier side chain of Thr helps maintain a structure that is closer to that found in wild type. For I200 (P2; Table 1), selectivity is altered little in I200V, but is lost in I200S and I200T, a result that parallels that with mutation of I94. I200L had significantly altered selectivity however (Table 1).

In the model (Fig. 7E, F), I94 points into a hydrophilic pocket, and I200 into a hydrophobic pocket. Polar substitutions of I94 (I94S, I94T) may interact with either T92 or T89 in the P1 pore helix. Comparison of crystal structures of KcsA in high and low potassium concentration shows that the equivalent Val in KcsA undergoes conformation change, dependent on $[K^+]$ [57]. Our modelling suggests that, along with backbone deviations, the side chain of I94 also changes conformation and we anticipate the possibility of a side chain hydrogen bond in the mutants I94S or I94T which would impede any such change of conformation. As we show below these mutations both slow the response to voltage and impede shutting under acidification. I200 points principally into a hydrophobic pocket, but in the mutants I200S and I200T, a hydrogen bond may form with T198, also potentially impeding movement.

I94 and 200: mutants that alter ionic selectivity affect gating by voltage—Mutants of I94 and I200 where channels show essentially unaltered ionic selectivity (Table 1; Fig. 7) respond to voltage much as wild type channels do (Fig. 8A, I94V). In contrast, mutants of I94 and I200 where selectivity against Na^+ is reduced (Fig. 8A, I94S) show a slowed response to voltage that is similar to that found in non-selective mutants of `GY(F)G`. Alterations in structure that cause loss of selectivity thus broadly correlate with alterations in the response to voltage.

Mutants of I94 and I200 that alter selectivity also affect the response to acidification—When hydrophilic residues (Ser, Thr) replace I94, with the resultant abolition of ionic selectivity, sensitivity to acidification is also lost (Table 2; Fig. 8C). However replacement of I94 with hydrophobic residues Leu or Val, where channels retain ionic selectivity, results in the retention of a near-wild type response to acidification (Table 2; Fig. 8B). Mutations of I200 also diminish the response to acidification, apparently even in the case of I200V (Table 2).

Evidently disruption of the selectivity filter causes loss of ionic selectivity, a slowing of the response to depolarisation, and a loss or radical alteration in acid sensitivity.

Other pore mutants—The effects on ionic selectivity and of the response to acidification are documented in supplementary Tables 1 & 2.

Mutations of the pore helices

The pore helix of potassium channels is important in stabilising the selectivity filter, through side chain-side chain interactions [15]. Part of this region contributes to the potassium consensus TxxTxGYG, but the P1 region of TASK-1 differs from most K^+ channels in having Val in place of the first Thr (position 90; Fig. 1A, D). The preceding residue (position 89, immediately before the consensus sequence) is Thr. Thus the sequence in TASK-1 is TV, rather than the more conventional VT. We now ask whether this deviation from a pattern that is strongly conserved in other K^+ channels is important for K^+ channel function in TASK-1.

Table 1 shows the effects of substituting T89 by Val and V90 by Thr. These mutations (T89V and V90T) alter selectivity slightly. Other substitutions of T89 by Ala or even more conservatively by Ser or of V90 by Ser do produce significant loss of selectivity against Na^+ (Table 1). Mutants of V90 (V90L, V90T) have relatively little effect on pH sensitivity, causing a shift in an alkaline direction (Table 2). The pH sensitivity of the T89S mutant is close to that of the wild type channel.

Interestingly however, substitution of T89 with the hydrophobic residues Ala or Val resulted in channels showing behaviour comparable to that seen with Y96F and G97A: substantial current over the physiological range, but an increase in current in alkaline conditions (Table 2). This finding suggests that T89 may play a role in acid sensing by TASK-1.

Mutations of the pore regions – the outer pore mouth

We have already shown that mutations of the putative proton sensing residue H98 in P1 [1, 33, 38] alter the selectivity of TASK-1 ion channels, though they do so with little change in response of currents to voltage (see for example Fig. 4 of ref [55]). Replacement of the equivalent residue (D204) in P2 also alters ionic selectivity [55]. In the outer mouth of the channel, we have also made mutations A100T in P1 and V206T in P2 as well as the double mutation A100T/V206T.

We made these mutations initially to test whether introduction of Thr residues at these positions, mimicking the situation in Kv channels, would raise the low affinity of TASK-1 for the K^+ channel blocker TEA^+ (tetraethylammonium ion), but found no detectable blockage of channels by 26mM or even by 90mM TEA^+ in either wild type or mutant channels (A100T, V206T or A100T/V206T; data not shown). Thus introduction of a ring of Thr residues, important for TEA^+ blockage of Kv channels (T449 in *Shaker* [35]), does not confer such blockage onto TASK-1.

Both mutations (A100T and V206T) altered ionic selectivity somewhat (Table 1) while the double mutation A100T/V206T gave channels where Rb^+ was essentially indistinguishable from K^+ and with substantial permeability for Na^+ (Table 1). Thus, alteration of the structure, even of the outer mouth of the channel alters the ionic selectivity of TASK-1.

In Kv channels residues in the equivalent positions also regulate C-type inactivation [34]. And in TASK-1, the mutants A100T and V206T both show altered pH sensitivity (Table 2). In the case of A100T, pH sensitivity is essentially lost (Fig. 8D). Thus residues in positions similar to those contributing to the regulation of C-type inactivation in Kv channels also appear to contribute to the regulation of the response to acidification.

DISCUSSION

We have shown that mutation of residues in the pore regions of TASK-1 modify both channel selectivity and the responses of channels to changes of membrane potential and of extracellular pH. Modification of ionic selectivity is to be expected given the established role of the P-region as selectivity filter. Our experiments confirm that both P1 and P2 contribute to this process. Further, most positions in these pore regions are tolerant of mutation in that most mutant channels conduct ions. This tolerance may occur partly because point mutations of TASK-1 result in only two residues being replaced at a given level in the selectivity filter, rather than four as in Kv or Kir. But then in contrast to the situation with Kv and Kir channels, most mutations, though producing channels that transported ions, abolished the ability to select among the ions transferred. The rather complex arrangement found in tandem pore channels, with subtle differences between P1 and P2, appears essential for selectivity. Unlike the situation in Kv and Kir, where the aromatic residue in GY(F)G may be replaced with conservation of K^+ selectivity [20, 47], even conservative replacements in TASK-1 – Tyr96 by Phe, Phe202 by Tyr – produce TASK channels that are non-selective among the monovalent cations studied. However, our results do not support the hypothesis of Chapman *et al.* [7] that Y96 and D204 in TASK-1 are the principal residues determining ionic selectivity in tandem pore channels. Nor do our results (or those of Lopes *et al.* [32]; see also [55]) suggest that TASK-1 – with F rather than Y in the `GY(F)G` triplet of P2 – has a less stringent K^+ selectivity than that of Kv channels [7].

Modification of the pore structure also leads to changes in the response of TASK-1 to voltage. The slowing of the response to depolarisation that occurs with such modification of structure appears reasonably well correlated with effects on ionic selectivity. Appropriate mutation of `IGY(F)G` in the pore itself slows the response to voltage and increases the amount of conductance change occurring under depolarisation. While modified ionic occupancy of the pore may be part of the mechanism, the results are consistent with the response to voltage being associated with a change in the conformation of the pore region. Such a conclusion puts this phenomenon in a class with that of gating at the selectivity filter [4], a class that includes C-type inactivation in Kv channels [34, 54] and the altered kinetics of Kir channels found in pore mutants [47]. Recently it has also been shown that voltage dependent gating of KcsA is associated with movements of the selectivity filter [10]. In KcsA this gating is driven by way of a charged residue (E71), the equivalent of T89 and I195 in TASK-1, which acts as voltage sensor, voltage dependence being lost in the mutant E71C. Though TASK-1 must sense voltage, we have not identified an individual residue playing a voltage sensing role. Nor have we quantified the equivalent charge associated with the process: this charge is likely to be small [32].

We have also shown that mutations in the pore helix or selectivity filter alter the response of the acid sensitive K^+ channel TASK-1 to changes of extracellular pH. It is well established that replacement of His98 weakens the pH sensitivity of TASK-1 and TASK-3 and this residue is thought to act as proton sensor [26, 44, 1, 33, 38]. However substitution of H98 is not the only replacement of an amino acid residue that causes loss or reduction of pH sensitivity. Our modelling of the TASK-1 structure indicates that the H98 side chain lies behind the selectivity filter of the channel rather than directly in the ion conduction pathway (Fig. 1C). Thus, protonation of the His side chain cannot simply cause channel blockage; rather such protonation must initiate a conformational change.

It is likely that this conformational change occurs principally at the selectivity filter. It has already been shown that the response to acidification is dependent on $[K^+]_o$ [32], suggesting that the permeant cation stabilises the open state, rather as has been described for C-type

inactivation in Kv channels [4, 54]. Involvement of the pore is supported by the fact that mutants of this region reduce or alter the response to acidification. The mutants G95A and I94S/T essentially abolish the response to acidification. In the X-ray structure of the bacterial channel KcsA, residues in the equivalent positions (G77 and V76 in KcsA) adopt different conformations in conducting and non-conducting states of the selectivity filter [57]; this suggests that G95 and I94 similarly adopt different conformations in open and shut states of TASK-1. At the outer mouth of the pore, residues in TASK-1 in positions equivalent to those controlling C-type inactivation in Kv channels – A100 in P1 and V206 in P2 – also help regulate the response to acidification. The mutant A100T is virtually completely unaffected by acidification, the channel appears to be stabilised in an open state in this mutant. On the basis of a likely common mechanism among potassium ion channels, these residues (G95, I94, A100) are in positions that might be expected to disrupt pH sensitivity if this response depends on a conformation change of the filter. However mutations of residues in other positions (Y96, F202, G97, etc) also radically alter the response to voltage.

Certain Kv channels respond to acidification, and this response is also thought to involve gating at the selectivity filter. Thus, in *Shaker* channels, extracellular acidification results in a marked acceleration of C-type inactivation [50]. Gating at the filter has also been proposed as the mechanism by which mammalian Kv1.4 [8, 31], 1.5 [23] and 1.3 [48] respond to low pH_o. Again, mutations that inhibit or slow C-type inactivation also inhibit sensitivity to extracellular pH. In these cases, a His residue in the extracellular linker controls entry to the outer mouth of the pore by acting as a proton sensor. This residue is H508 in Kv1.4 [8, 31]. As with H98 in TASK-1, modelling suggests that H508 lies adjacent to, but not directly in, the ion conduction pathway [8]. A His residue conserved in TASK channels in the M1-P1 linker (residue H72 in TASK-1, -3 and -5) is not involved in pH sensitivity of TASK-3 [26, 44], whilst in TASK-1, the mutant H72N has increased acid sensitivity [38]. A gating response to acidification has also been demonstrated for KCNQ2/3 K^+ channels [43]. Thus the response of TASK channels to acidification may share mechanism with K^+ channels of the Kv family.

We propose that H98 does indeed act as the proton sensor, with its protonation effecting a conformational change of the selectivity filter. The model of the TASK-1 channel suggests a mechanism that may partly explain how this process might occur. In more alkaline conditions, the unprotonated His side chain stabilises a water molecule at the back of the filter through an H-bond, with the water as donor. The water accepts two hydrogen bonds in turn from the backbone amides of Y96 and G97 in the selectivity filter (P1), while donating a further bond to the side chain of T89 (whose replacement does indeed alter the response to acidification; Table 2). These interactions are illustrated in supplementary Fig. 2. Protonation of H98 prevents this residue from accepting the hydrogen bond from the water molecule. As a result the water molecule may be destabilised, reducing its interactions with the backbone of the selectivity filter. A water molecule has similarly been described as stabilising the filter of KcsA in structures from X-ray crystallography [9].

In summary our results illustrate the effects of a number of pore mutations on ionic selectivity. Both P1 and P2 contribute to selectivity and the subtle differences that exist between P1 and P2 appear necessary for ionic selectivity. Several mutations that affect ionic selectivity also slow the response of the channel to depolarisation. This response is then likely to be associated with a change in conformation of the pore. So also is the response to acidification, since pore mutations also reduce or radically alter this important physiological response. Our results are consistent with H98 in the pore mouth acting as a proton sensor. However, such protonation must initiate a gating response that involves conformational change in the selectivity filter of this channel.

Supplementary Material

Refer to Web version on PubMed Central for supplementary material.

Acknowledgments

We thank the BBSRC and the Wellcome Trust for support. P.J.S. is supported by a MRC/Novartis CASE Studentship.

REFERENCES

1. Ashmole I, Goodwin PA, Stanfield PR. TASK-5, a novel member of the tandem pore K^+ channel family. Pflügers Arch. 2001; 442:828–833.
2. Bayliss DA, Talley EM, Siros JE, Lei Q. TASK-1 is a highly modulated pH-sensitive 'leak' K^+ channel expressed in brainstem respiratory neurons. Respir Physiol. 2001; 129:159–174. [PubMed: 11738652]
3. Bezanilla F, Armstrong CM. Negative conductance caused by entry of sodium and cesium ions into the potassium channels of squid axons. J Gen Physiol. 1972; 60:588–608. [PubMed: 4644327]
4. Bichet D, Haass FA, Jan LY. Merging functional studies with structures of inward-rectifier K^+ channels. Nat Rev Neurosci. 2003; 4:957–967. [PubMed: 14618155]
5. Bockenhauer D, Zilberberg N, Goldstein SAN. KCNK2: reversible conversion of a hippocampal leak into a voltage-dependent channel. Nature Neurosci. 2001; 4:486–491. [PubMed: 11319556]
6. Buckler KJ, Williams BA, Honoré E. An oxygen-, acid- and anaesthetic- sensitive TASK-like background potassium channel in rat arterial chemo-receptor cells. J Physiol. 2000; 525:135–142. [PubMed: 10811732]
7. Chapman ML, Krovetz HS, VanDongen AMJ. GYGD pore motifs in neighbouring potassium channel subunits interact to determine ion selectivity. J Physiol. 2001; 530:21–33. [PubMed: 11136855]
8. Claydon TW, Boyett MR, Sivaprasadarao A, Orchard CH. Two pore residues mediate acidosis-induced enhancement of C-type inactivation of the Kv1.4 K^+ channel. Am J Physiol. 2002; 283:C1114–C1121.
9. Cordero-Morales JF, Cuello LG, Zhao YX, Jogini V, Cortes DM, Roux B, Perozo E. Molecular determinants of gating at the potassium-channel selectivity filter. Nat Struct Mol Biol. 2006a; 13:311–318. [PubMed: 16532009]
10. Cordero-Morales JF, Cuello LG, Perozo E. Voltage dependent gating at the KcsA selectivity filter. Nat Struct Mol Biol. 2006b; 13:319–322. [PubMed: 16532008]
11. Czirják G, Petheo GL, Spat A, Enyedi P. Inhibition of TASK-1 potassium channel by phospholipase C. Am J Physiol. 2001; 281:C700–708.
12. Czirják G, Toth ZE, Enyedi P. The two-pore domain K channel, TRESK, is activated by the cytoplasmic calcium signal through calcineurin. J Biol Chem. 2004; 279:18550–18558. [PubMed: 14981085]
13. Decher N, Maier M, Dittrich W, Gassenhuber J, Bruggemann A, Busch AE, Steinmeyer K. Characterization of TASK-4, a novel member of the pH-sensitive, two-pore domain potassium channel family. FEBS Lett. 2001; 492:84–89. [PubMed: 11248242]
14. DeLano WL. The PyMOL molecular Graphics System. 2002http://www.pymol.org
15. Doyle DA, Morais Cabral J, Pfuetzner RA, Kuo A, Gulbuis JM, Cohen SL, Chait BT, MacKinnon R. The structure of the potassium channel: molecular basis of K^+ conduction and selectivity. Science. 1998; 280:69–77. [PubMed: 9525859]
16. Duprat F, Lesage F, Fink M, Reyes R, Heurteaux C, Lazdunski M. TASK, a human background K^+ channel to sense external pH variations near physiological pH. EMBO J. 1997; 16:5464–5471. [PubMed: 9312005]
17. Girard C, Duprat F, Terrenoire C, Tinel N, Fosset M, Romey G, Lazdunski M, Lesage F. Genomic and functional characteristics of novel human pancreatic 2P domain K^+ channels. Biochem. Biophys. Res. Commun. 2001; 282:249–256. [PubMed: 11263999]

18. Goldstein SA, Bockenhauer D, O'Kelly I, Zilberberg N. Potassium leak channels and the KCNK family of two-P-domain subunits. Nat Rev Neurosci. 2001; 2:175–184. [PubMed: 11256078]
19. Hadjú P, Ulens C, Panyi G, Tytgat J. Drug- and mutagenesis-induced changes in the selectivity filter of a cardiac two-pore background K^+ channel. Cardiovasc Res. 2003; 58:46–54. [PubMed: 12667945]
20. Heginbotham L, Lu Z, Abramson T, MacKinnon R. Mutations in the K^+ channel signature sequence. Biophys J. 1994; 66:1061–1067. [PubMed: 8038378]
21. Jentsch TJ, Poët M, Fuhrmann JC, Zdebik AA. Physiological functions of CLC Cl^- channels gleaned from human genetic disease and mouse models. Ann Rev Physiol. 2005; 67:779–807. [PubMed: 15709978]
22. Karschin C, Wischmeyer E, Preisig-Muller R, Rajan S, Derst C, Grzeschik KH, Daut J, Karschin A. Expression pattern in brain of TASK-1, TASK-3, and a tandem pore domain K^+ channel subunit, TASK-5, associated with the central auditory nervous system. Mol Cell Neurosci. 2001; 18:632–648. [PubMed: 11749039]
23. Kehl SJ, Eduljee C, Kwan DC, Zhang S, Fedida D. Molecular determinants of the inhibition of human Kv1.5 potassium currents by external protons and Zn^{2+} J Physiol. 2002; 541:9–24. [PubMed: 12015417]
24. Kim D, Fujita A, Horio Y, Kurachi Y. Cloning and functional expression of a novel cardiac two-pore background K^+ channel (cTBAK-1). Circ Res. 1998; 82:513–518. [PubMed: 9506712]
25. Kim D, Gnatenco C. TASK-5, a new member of the tandem-pore K^+ channel family. Biochem Biophys Res Commun. 2001; 284:923–930. [PubMed: 11409881]
26. Kim Y, Bang H, Kim D. TASK-3 a novel member of the tandem pore K^+ channel family. J Biol Chem. 2000; 275:9340–9347. [PubMed: 10734076]
27. Lauritzen I, Zanzouri M, Honore E, Duprat F, Ehrengruber MU, Lasdunski M, Patel AJ. K^+-dependent cerebellar granule neuron apoptosis. Role of TASK leak K^+ channels. J Biol Chem. 2003; 278:32068–32076. [PubMed: 12783883]
28. Leonoudakis D, Gray AT, Winegar BD, Kindler CH, Harada M, Taylor DM, Chavez RA, Forsayeth JR, Yost CS. An open rectifier potassium channel with two pore domains in tandem cloned from rat cerebellum. J Neurosci. 1998; 18:868–877. [PubMed: 9437008]
29. Lesage F, Lazdunski M. Molecular and functional properties of two-pore-domain potassium channels. Am J Physiol Renal Physiol. 2000; 279:F793–F801. [PubMed: 11053038]
30. Lesage F, Reyes R, Fink M, Duprat F, Guillemare E, Lazdunski M. Dimerization of TWIK-1 K+ channel subunits via a disulfide bridge. EMBO J. 1996; 15:6400–6407. [PubMed: 8978667]
31. Li X, Bett GC, Jiang X, Bondarenko VE, Morales MJ, Rasmusson RL. Regulation of N- and C-type inactivation of Kv1.4 by pH_o and K^+: evidence for transmembrane communication. Am J Physiol. 2003; 284:H71–H80.
32. Lopes CMB, Gallagher PG, Buck ME, Butler MH, Goldstein SAN. Proton block and voltage gating are potassium dependent in the cardiac leak channel Kcnk3. J Biol Chem. 2000; 275:16969–16978. [PubMed: 10748056]
33. Lopes CMB, Zilberberg N, Goldstein SAN. Block of Kcnk3 by protons. J Biol Chem. 2001; 276:24449–24452. [PubMed: 11358956]
34. Lopez-Barneo J, Hoshi T, Heinemann SH, Aldrich RW. Effects of external cations and mutations in the pore region on C-type inactivation of Shaker potassium channels. Receptors Channels. 1993; 1:61–71. [PubMed: 8081712]
35. MacKinnon R, Yellen G. Mutations affecting TEA blockade and ion permeation in voltage-activated K^+ channels. Science. 1990; 250:276–279. [PubMed: 2218530]
36. McGuffin LJ, Bryson K, Jones DT. The PSIPRED protein structure prediction server. Bioinformatics. 2000; 16:404–405. [PubMed: 10869041]
37. Maingret F, Honoré E, Lazdunski M, Patel AJ. Molecular basis of the voltage dependent gating of TREK-1, a mechano-sensitive K^+ channel. Biochem Biophys Res Comm. 2002; 292:339–346. [PubMed: 11906167]
38. Morton MJ, O'Connell AD, Sivaprasadarao A, Hunter M. Determinants of pH sensing in the two-pore domain K^+ channels TASK-1 and -2. Pflügers Archiv. 2003; 445:557–583.

39. O'Connell AD, Morton MJ, Sivaprasadarao A, Hunter M. Selectivity and interactions of Ba^{2+} and Cs^{+} with wild-type and mutant TASK1 K^{+} channels expressed in *Xenopus* oocytes. J Physiol. 2004; 562:687–696. [PubMed: 15611021]
40. Passmore, G. Structure-function studies of inwardly rectifying potassium channels. University of Leicester; 2003. PhD Thesis
41. Patel AJ, Honoré E. Properties and modulation of mammalian 2P domain K^{+} channels. Trends Neurosci. 2001; 24:339–346. [PubMed: 11356506]
42. Pei L, Wiser O, Slavin A, Mu D, Powers S, Jan LY, Hoey T. Oncogenic potential of TASK3 (Kcnk9) depends on K^{+} channel function. Proc Natl Acad Sci. 2003; 100:7803–7807. [PubMed: 12782791]
43. Prole DL, Lima PA, Marrion NV. Mechanisms underlying modulation of neuronal KCNQ2/KCNQ3 potassium channels by extracellular protons. J Gen Physiol. 2003; 122:775–793. [PubMed: 14638935]
44. Rajan S, Wischmeyer E, Xin Liu G, Preisig-Muller R, Daut J, Karschin A, Derst C. TASK-3, a novel tandem pore domain acid-sensitive K^{+} channel. An extracellular histidine as pH sensor. J Biol Chem. 2000; 275:16650–16657. [PubMed: 10747866]
45. Reyes R, Duprat F, Lesage F, Fink M, Salinas M, Farman N, Lazdunski M. Cloning and expression of a novel pH-sensitive two pore domain K^{+} channel from human kidney. J Biol Chem. 1998; 273:30863–30869. [PubMed: 9812978]
46. Sali A, Blundell TL. Comparative protein modelling by satisfaction of spatial restraints. J Mol Biol. 1993; 234:779–815. [PubMed: 8254673]
47. So I, Ashmole I, Davies NW, Sutcliffe MJ, Stanfield PR. The K^{+} channel signature sequence of murine Kir2.1: mutations that affect microscopic gating but not ionic selectivity. J Physiol. 2001; 531:37–50. [PubMed: 11179390]
48. Somodi S, Varga Z, Hadju P, Starkus JG, Levy DI, Gaspar R, Panyi G. pH-dependent modulation of Kv1.3 inactivation: role of His399. Am J Physiol. 2004; 287:C1067–C1076.
49. Stanfield PR, Nakajima S, Nakajima Y. Constitutively active and G-protein coupled inward rectifier K^{+} channels: Kir2.0 and Kir3.0. Rev Physiol Biochem Pharmacol. 2002; 145:47–179. [PubMed: 12224528]
50. Starkus JG, Varga Z, Schonherr R, Heinemann SH. Mechanisms of the inhibition of Shaker potassium channels by protons. Pflügers Arch. 2003; 447:44–54.
51. Taglialatela M, Drew LA, Kirsch GE, de Biasi M, Hartmann HA, Brown AM. Regulations of K^{+}/Rb^{+} selectivity and internal TEA blockade by mutations at a single site in K^{+} pores. Pflügers Arch. 1993; 423:104–112.
52. Tosatto SC, Bindewald E, Hesser J, Manner R. A divide and conquer approach to fast loop modelling. Protein Eng. 2001; 15:279–86. [PubMed: 11983928]
53. Wood ZA, Poole LB, Karplus PA. Structure of intact AhpF reveals a mirrored thioredoxin-like active site and implies large domain rotations during catalysis. Biochemistry. 2001; 40:3900–11. [PubMed: 11300769]
54. Yellen G. The moving parts of voltage-gated ion channels. Q Rev Biophys. 1998; 31:239–295. [PubMed: 10384687]
55. Yuill KH, Ashmole I, Stanfield PR. The selectivity filter of the tandem pore potassium channel TASK-1 and its pH sensitivity and ionic selectivity. Pflügers Arch. 2004; 448:63–69.
56. Zilberberg N, Iloan N, Goldstein SAN. KCNK0: opening and closing the 2-P-domain potassium leak channel entails ‘C-type’ gating of the outer pore. Neuron. 2001; 32:635–648. [PubMed: 11719204]
57. Zhou Y, Morais-Cabral JH, Kaufman A, MacKinnon R. Chemistry of ion coordination and hydration revealed by a K^{+} channel-*Fab* complex at 2.0Å resolution. Nature. 2001; 414:23–24. [PubMed: 11689922]

Europe PMC Funders Author Manuscripts

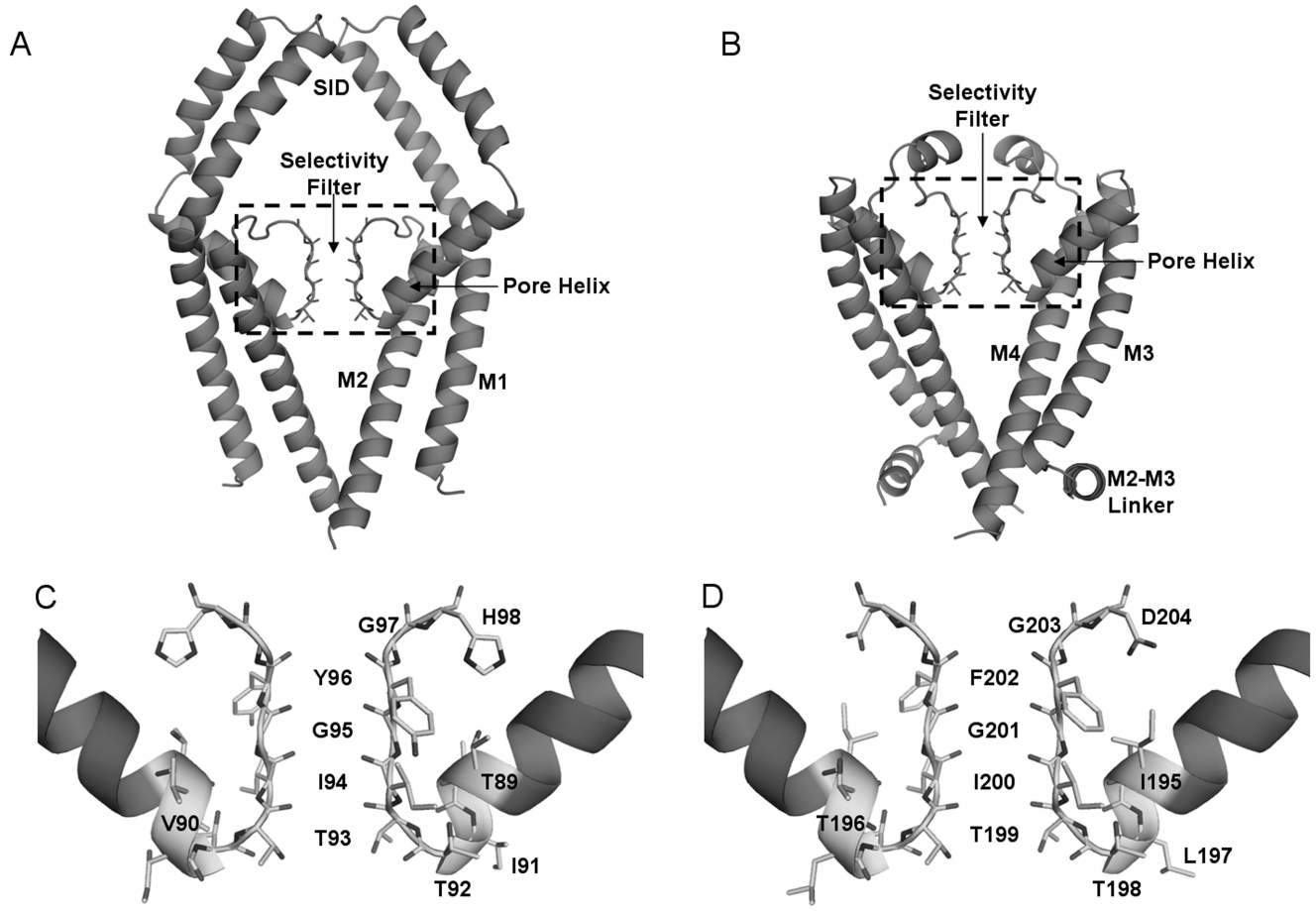

Figure 1.

Homology model of the TASK-1 Channel

A. The P1 segment of the TASK-1 homology model. B. The P2 segment of the TASK-1 homology model. The region shown in C. and D. is highlighted by a dashed box. C. The residues within the pore helices and selectivity filter of P1. D. The residues within the pore helices and selectivity filter of P2.

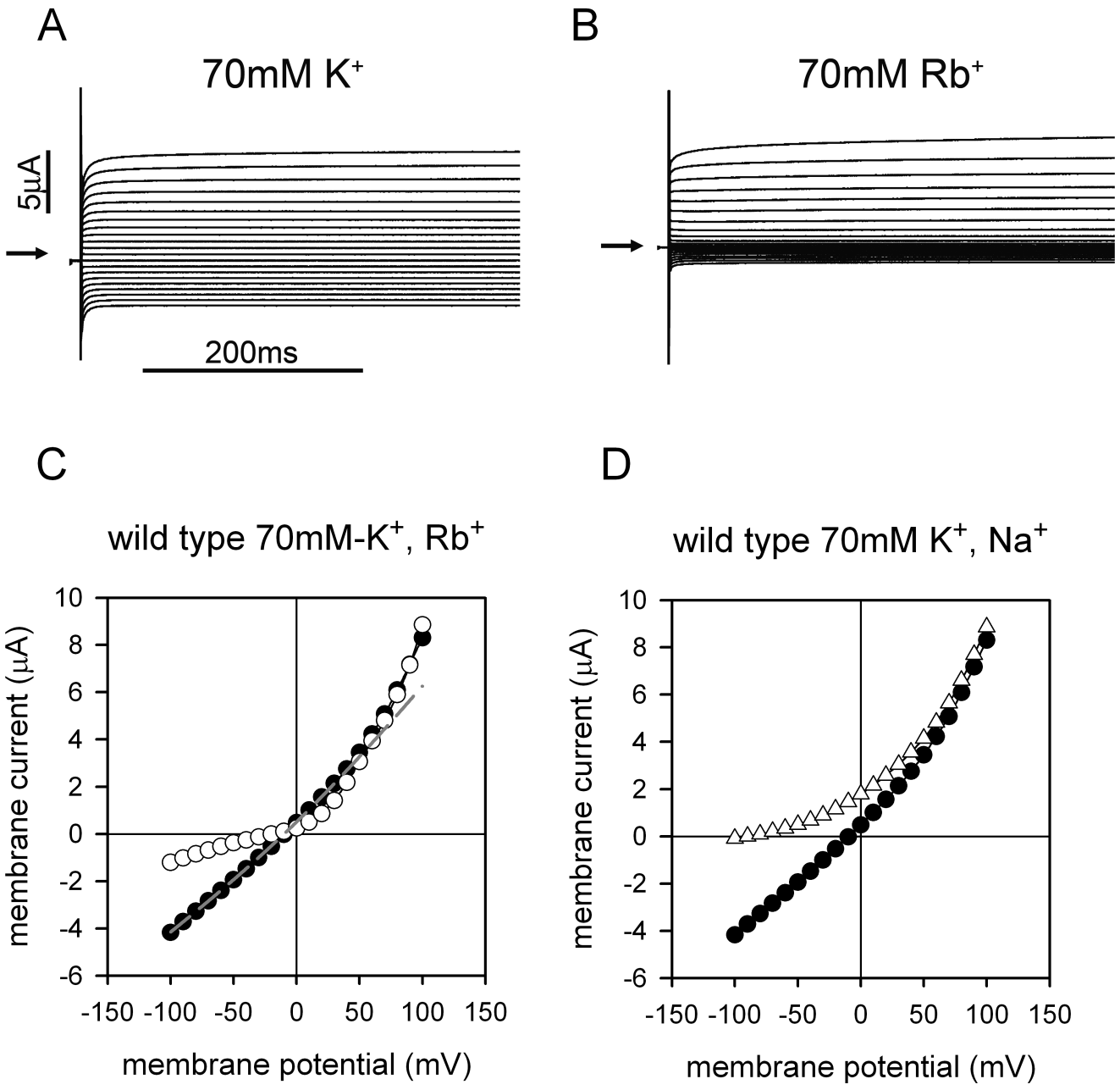

Figure 2.

Ionic selectivity of wild type channels.

A, B Current records for wild type in 70mM $[K^+]_o$ (A) and in 70mM $[Rb^+]_o$ solutions (B). The membrane was held at −20mV and stepped in 10mV increments to between −100 and +100mV. The horizontal arrows show the zero current level.

C. Current voltage relations measured in a *Xenopus* oocyte expressing wild type TASK-1 in solutions containing 70mM $[K^+]_o$ (●) and 70mM $[Rb^+]_o$ (○). Rb^+ reduced outward K^+ current under depolarisations up to +80mV. The dashed grey line is computed by fitting the hyperpolarising element of the current voltage relation in K^+ solution with the constant field

equation $I_K = P_K \frac{VF^2}{RT} \left\{ \frac{[K^+]_o . \exp(VF/RT) - [K^+]_i}{\exp(VF/RT) - 1} \right\}$ and extrapolating over the depolarising region. Outward currents are larger than predicted owing to a voltage- and time-dependent increase in current under depolarisation. D. Current voltage relations in 70mM $[K^+]_o$ (●) and 70mM $[Na^+]_o$ (△).

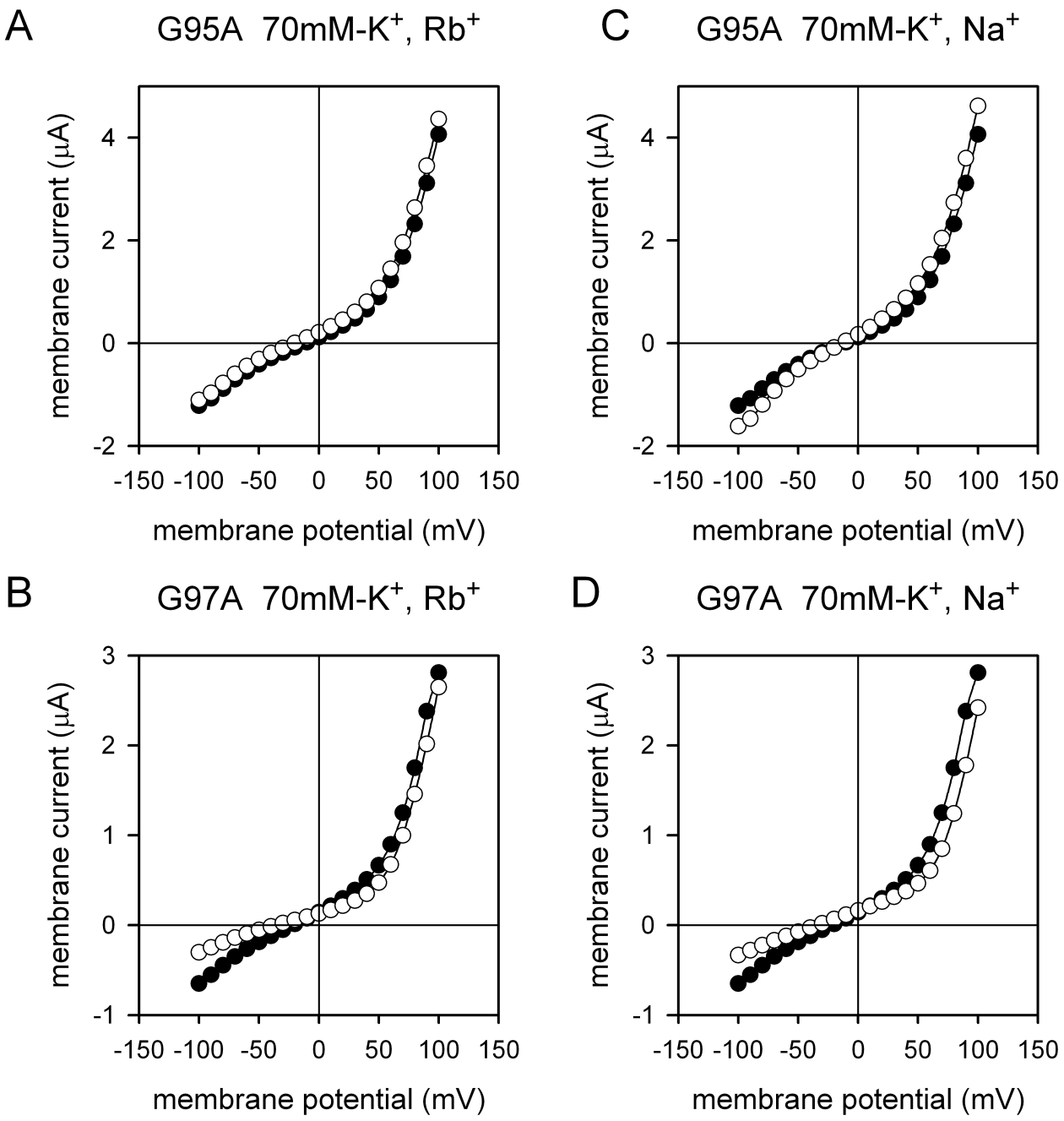

Figure 3.

Mutation of the glycine residues of the GY(F)G triplet and ionic selectivity.

Typical current voltage relations from individual oocytes expressing the TASK-1 mutants: A, G95A in 70mM $[K^+]_o$ (●) and in 70mM $[Rb^+]_o$ (○); B, G97A in 70mM $[K^+]_o$ (●) and in 70mM $[Rb^+]_o$ (○) C, G95A in70mM $[K^+]_o$ (●) and in 70mM $[Na^+]_o$ (○) ; and D, G97A in 70mM $[K^+]_o$ (●) and in 70mM $[Na^+]_o$ (○) showing resultant loss of selectivity.

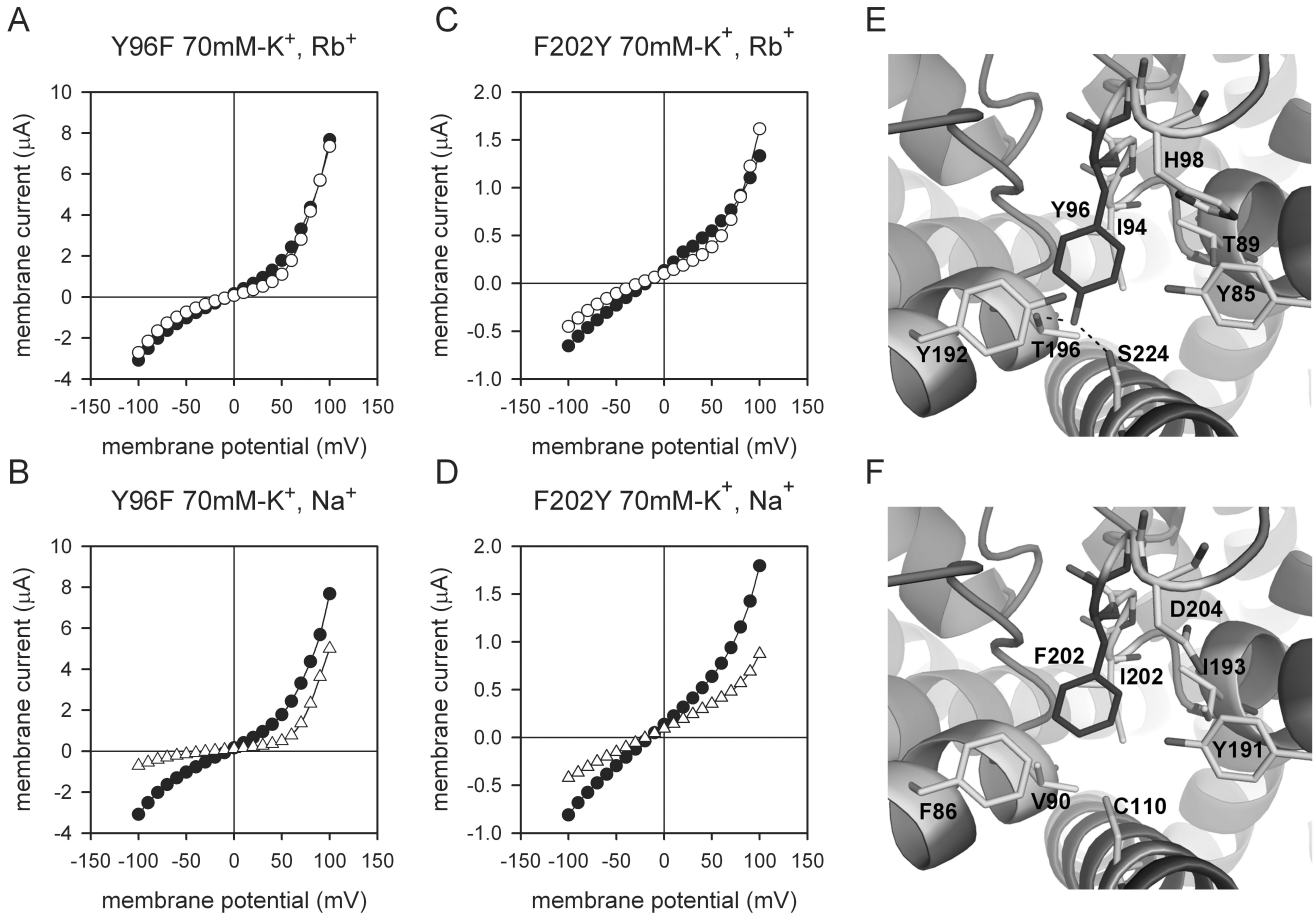

Figure 4.

Mutation Y96 and F202 of the GY(F)G triplet and ionic selectivity.

Typical current voltage relations from individual oocytes expressing the TASK-1 mutants: A, Y96F in 70mM $[K^+]_o$ (●) and in 70mM $[Rb^+]_o$ (○); B, Y96F in 70mM $[K^+]_o$ (●) and in 70mM $[Na^+]_o$ (△);C, F202Y in 70mM $[K^+]_o$ (●) and in 70mM $[Rb^+]_o$ (○); D, F202Y in 70mM $[K^+]_o$ (●) and in 70mM $[Na^+]_o$ (△); E and F. Potential interactions behind the selectivity filter suggested by our modelling studies (E) Y96 (P1) may form hydrogen bonds with T196 and S224 (depicted by dashed lines). (F) F202 (P2) is in a more hydrophobic environment than the equivalent residue in P1 (Y96), consistent with the loss of the hydroxyl. F86, V90, C110, Y191, I195, I200 and D204 surround F202.

Europe PMC Funders Author Manuscripts

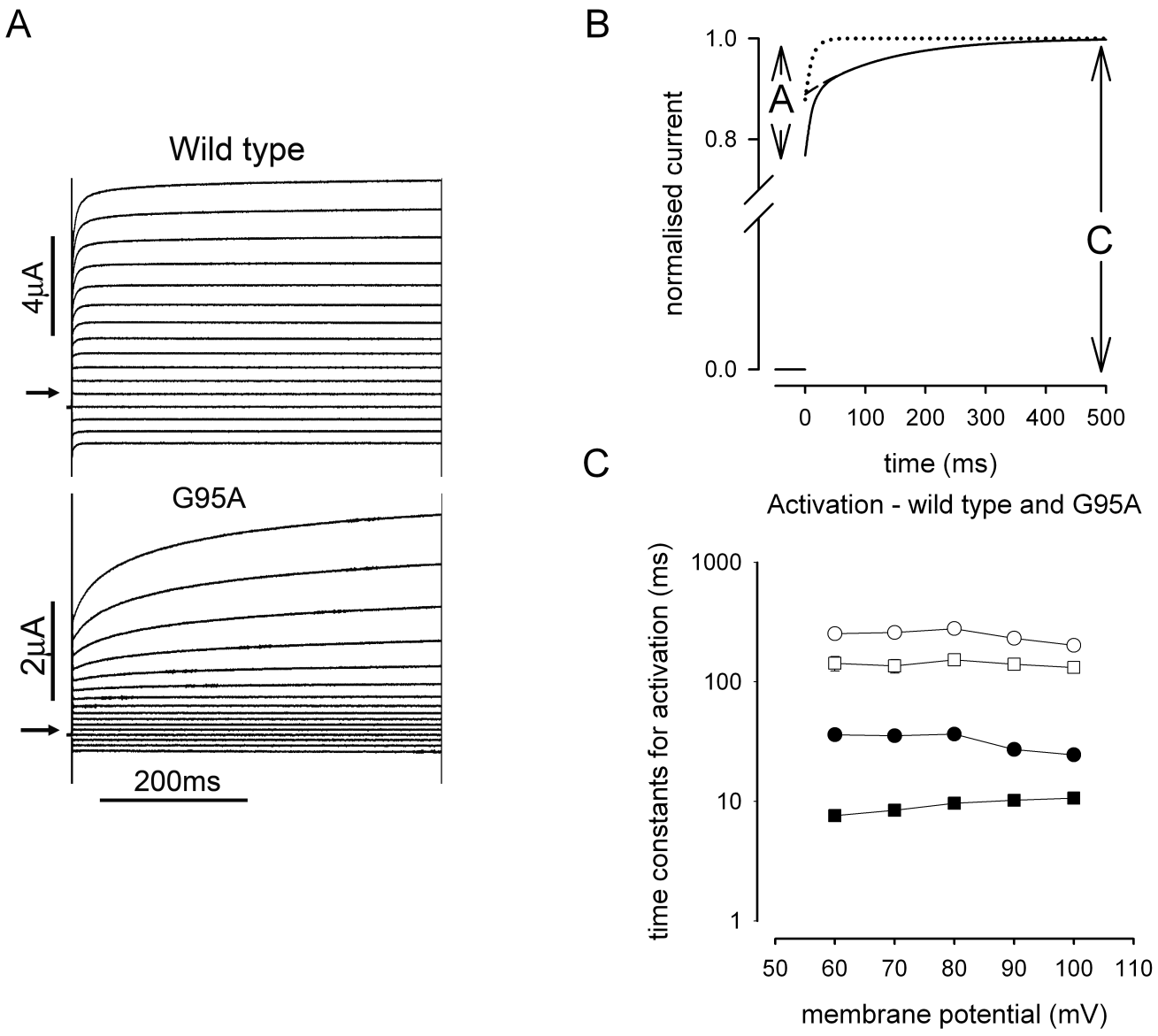

Figure 5.

Mutations of the selectivity filter alter voltage dependent gating.

A. Records of currents recorded from oocytes expressing wild type (above) and G95A TASK-1. External solutions contain 70mM K^+ and currents were recorded under voltage steps in increments of 10mV from a holding potential of −20mV to between +100mV and −100mV. For clarity we have illustrated records from +100 to −50mV. B. Currents were fit with an expression (also given as Eqn (3) of the text) describing activation of current with two exponential components: $I_K(t) = A_1.\exp(-t/\tau_1) + A_2.\exp(-t/\tau_2) + C$. In the text, the fraction of the current activated by the depolarisation is computed by the quantity A/C as illustrated. The fast and slow components are indicated as the dotted and the dashed lines, respectively. The mean values from the fits to wild type currents were used to compute the diagram. C. Plot of activation time constants τ_1 (■ for wild type and ● for G95A) and τ_2 (□ for wild type and ○ for G95A) against voltage obtained by fitting currents as in B. Error bars indicate ± s.e.m. Both elements of activation are significantly slowed in the mutant channel

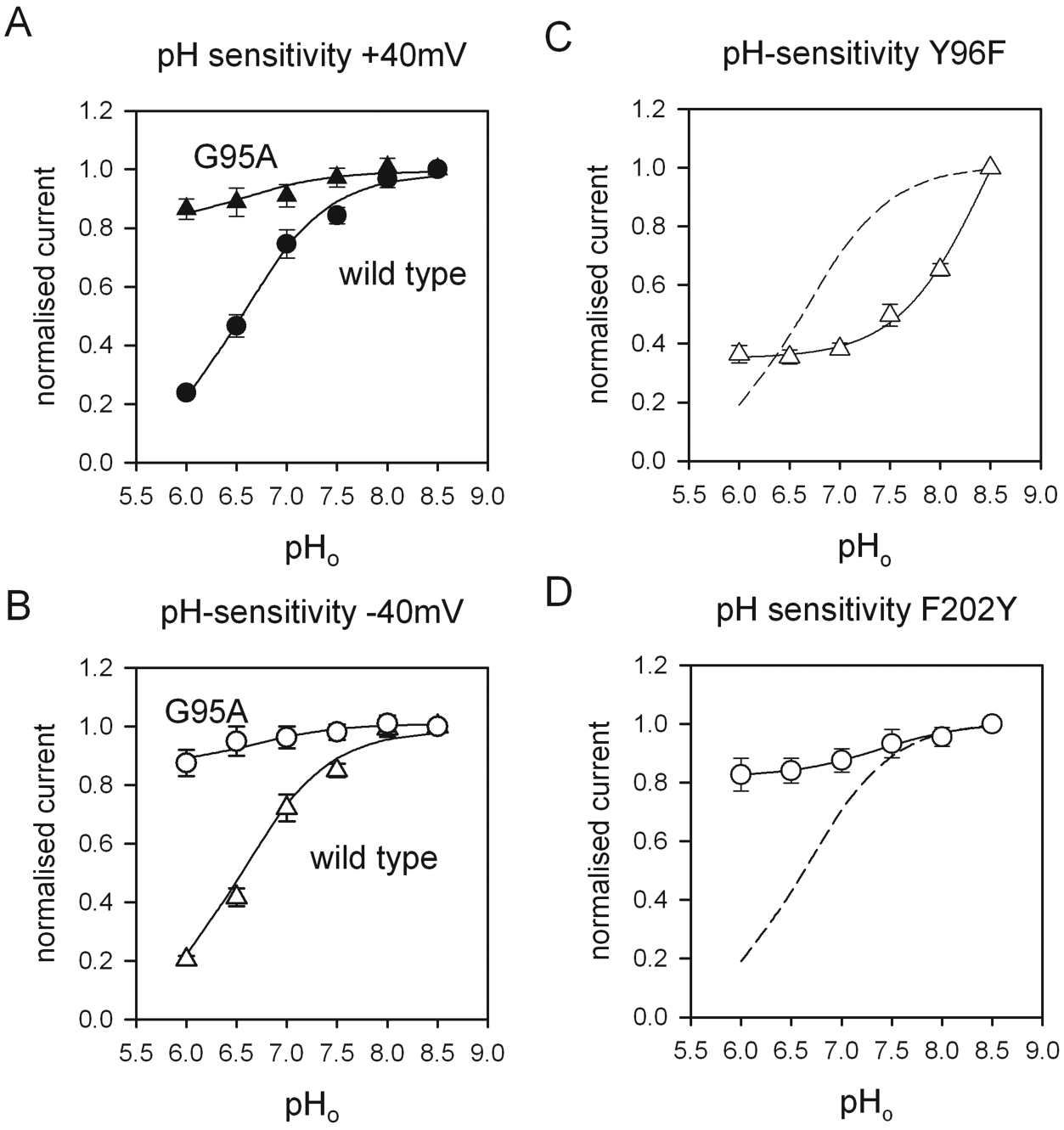

Figure 6.

Response to acidification of wild type TASK-1 wild type and of selectivity filter mutants. A. Relationship between the membrane current, normalised to that at pH_o = 8.5, (ordinate) and pH_o (abscissa) for wild type (●) and G95A (▲), measured at +40mV. The points give the mean ± s.e.m. in each case. The lines are drawn using Eqn (2) of the text, that is to:

$y=a.\left\{1+\frac{[H^+]_o}{K_a}\right\}^{-1}+b$. In both cases, pK_a = 6.54 (best fit to the mean results for wild type). For G95A, a = 0.14, b = 0.86. B. Relationship between membrane current and pH_o, as in A but measured at −40mV for wild type (○) and G95A (△). Lines are drawn using Eqn (2)

with pK_a = 6.64; for G95A, a = 0.19, b = 0.81. C. Similar relationships for Y96F at −40mV (△). The solid line gives pK_a = 8.46, a = 1.23, b = 0.35 for the fit to −40mV. D. Similar relationships for F202Y at −40mV (○). The solid line gives pK_a = 7.36, a = 0.18, b = 0.82 for the fit to −40mV. For parts C and D, the dashed line gives the best fit to wild type at −40mV (as in B).

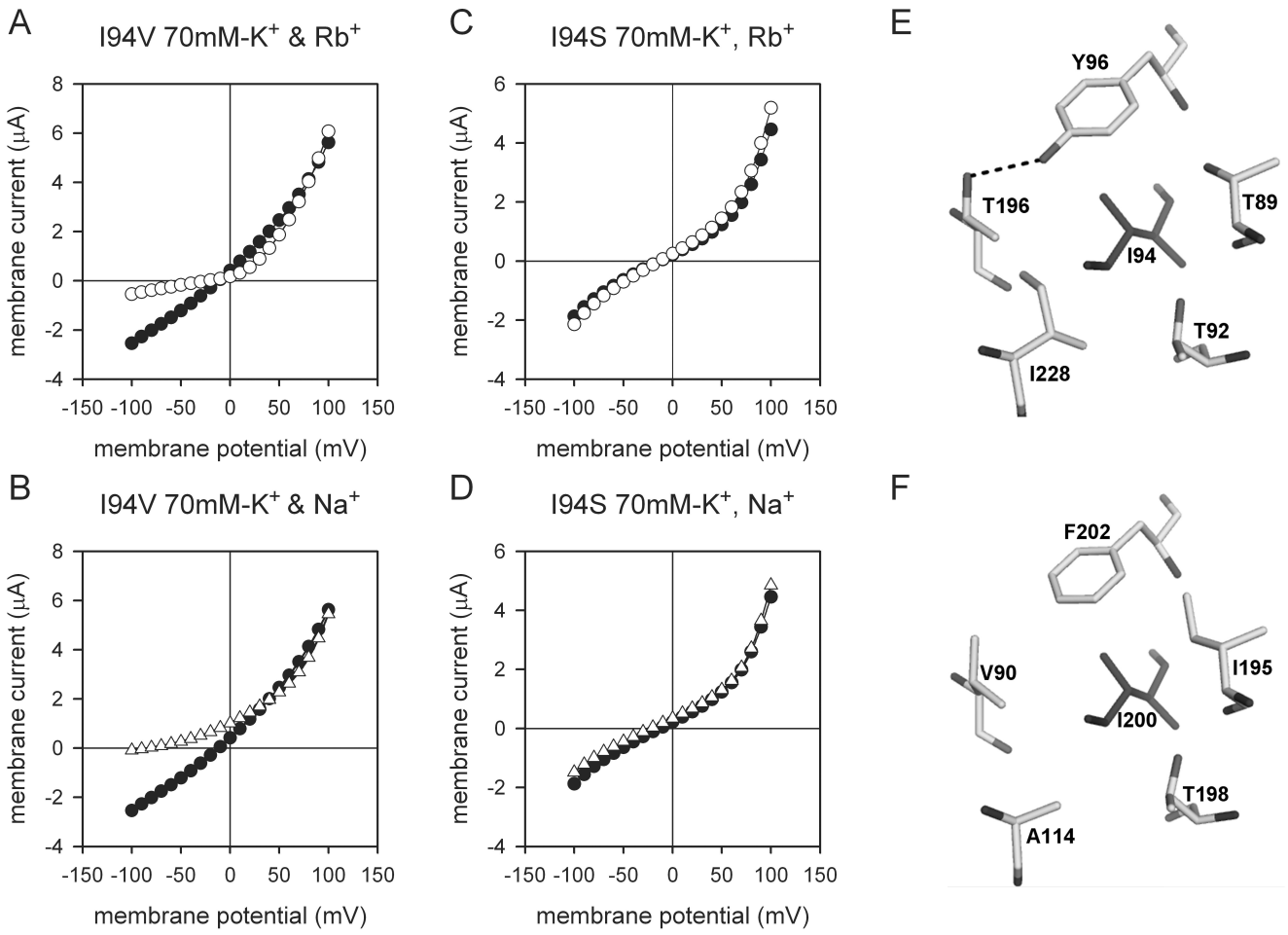

Figure 7.

Mutations of I94 in the consensus sequences of P1.

A and B. Current voltage relations for the P1 mutant I94V in (A), 70mM $[K^+]_o$ (●) and in 70mM $[Rb^+]_o$ (○); and (B), 70mM $[K^+]_o$ (●) and in 70mM $[Na^+]_o$ (△); channels retain some selectivity in this mutant. C and D. Current voltage relations for I94S under similar experimental conditions (K^+, ●; Rb^+, ○; Na^+, △); channels lose ionic selectivity with this less conservative mutation. E and F. Potential interactions of I94 and its equivalent in P2, I200 suggested by our modelling studies. The residues behind the selectivity filter, surrounding I94 (E); the residues behind the selectivity filter, surrounding I200 (F).

Europe PMC Funders Author Manuscripts

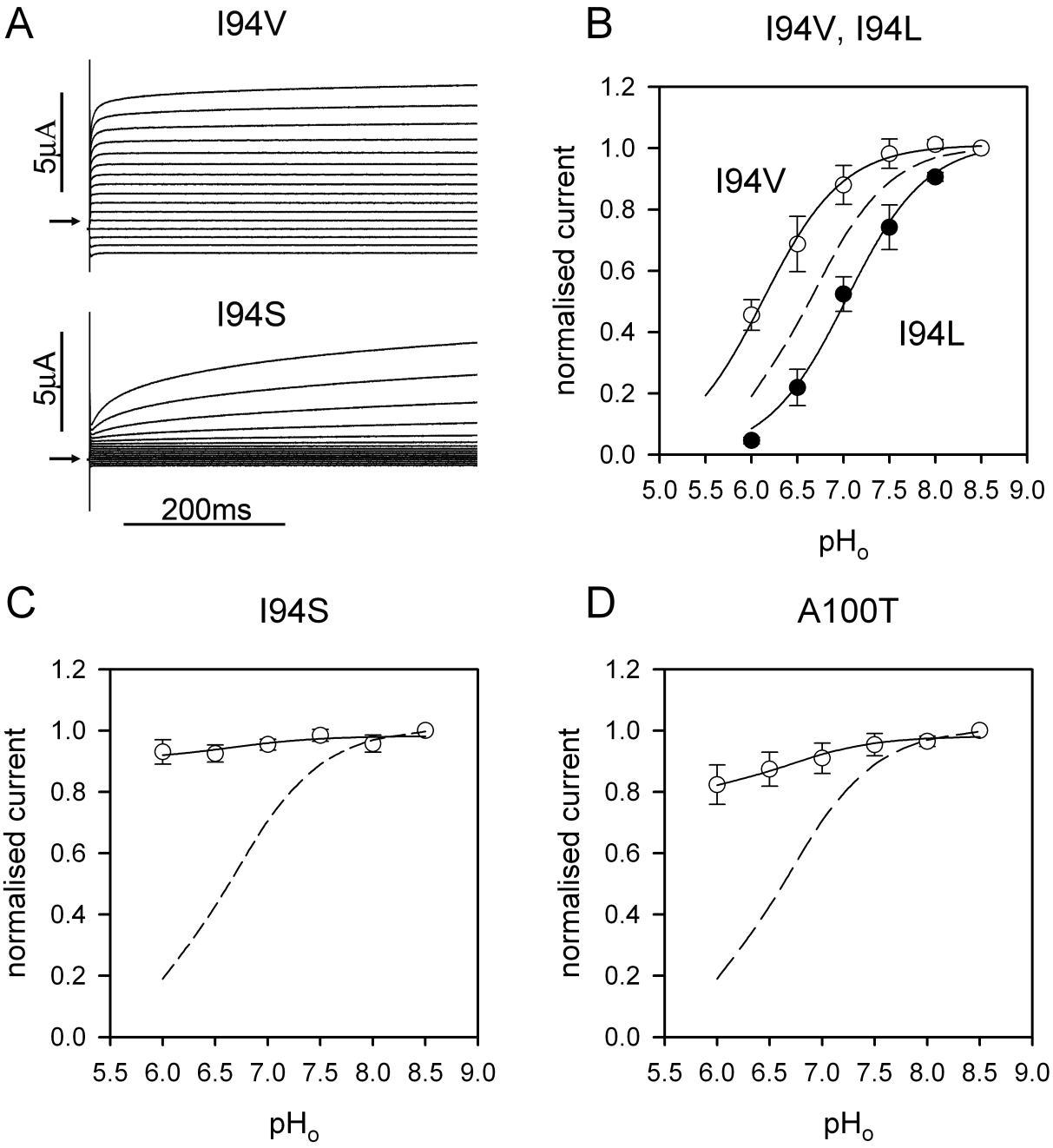

Figure 8.

Mutations of I94 gating by voltage and changes in extracellular pH.

A. Records of currents recorded from oocytes expressing I94V (above) and I94S (below) TASK-1. External solutions contain 70mM K^+ and currents were recorded under voltage steps in increments of 10mV from a holding potential of −20mV to between +100mV and −50mV. B. Relationship between the membrane current, normalised to that at pH_o = 8.5, (ordinate) and pH_o (abscissa) for I94V (○) and I94L (●), measured at −40mV. The solid line gives the fit of Eqn (2) to the values at −40mV, with pK_a = 6.13 for I94V and 7.04 for I94L. For all parts of this figure, the dashed line gives the best fit to wild type at −40mV (as in Fig. 6B). C. Similar relationships for I94S at −40mV (○). For I94S at −40mV, the solid

line gives pK_a = 6.54 (from wild type) and a = 0.08, b = 0.92. D. Similar relationships for A100T −40mV (○). The solid line gives pK_a = 6.64 (from wild type), a = 0.20, b = 0.78 for the fit to −40mV.

Europe PMC Funders Author Manuscripts

Europe PMC Funders Author Manuscripts

Pflugers Arch. Author manuscript; available in PMC 2008 July 31.

Table 1

Relative permeabilities to Rb^+ and Na^+ of mutants of the selectivity filters of P1 and P2

	Rb^+			Na^+		
	ΔE_{rev}	P_{Rb}/P_K	I_{Rb}/I_K(−100mV)	ΔE_{rev}	P_{Na}/P_K	I_{Na}/I_K(−100mV)
Wild type	−6.78 ± 1.02 (9)	0.77 ± 0.03 (9)	0.27 ± 0.02 (9)	−84.54 ± 2.32 (16)	0.04 ± 0.003 (16)	0.02 ± 0.01 (9)
Mutant	Selectivity filter – P1					
I94L	−6.88 ± 0.55 (4)	0.76 ± 0.02 (4)	0.53 ± 0.05 (4)	−83.45 ± 11.24 (4)	0.05 ± 0.02 (4)	0.01 ± 0.01 (4)
I94V	−10.38 ± 0.79 (5)	0.66 ± 0.03 (5)	0.29 ± 0.04 (5)	−73.48 ± 4.55 (5)	0.06 ± 0.01 (5)	0.03 ± 0.01 (5)
I94S	−1.01 ± 1.11 (8) **	0.97 ± 0.05 (8)	1.04 ± 0.08 (8) **	−11.21 ± 2.47 (8) **	0.66 ± 0.06 (8)	0.75 ± 0.05 (8) **
I94T	−2.33 ± 1.37 (3)	0.91 ± 0.05 (3)	1.14 ± 0.14 (3) **	−28.13 ± 6.91 (3) **	0.35 ± 0.09 (3)	0.33 ± 0.15 (3)
G95A	−3.06 ± 0.57 (14)	0.89 ± 0.02 (14)	0.91 ±0.05 (14) **	−3.96 ± 1.63 (8) **	0.87 ± 0.06 (8)	0.95 ± 0.09 (8) **
G95D	−5.82 ± 1.18 (11)	0.80 ± 0.04 (11)	0.64 ± 0.05 (11) **	−6.88 ± 1.95 (6) **	0.77 ± 0.06 (6)	0.60 ± 0.11 (6) **
G95D/WT	−9.14 ± 2.34 (5)	0.71 ± 0.06 (5)	0.63 ± 0.09 (5) *	−18.82 ± 5.30 (5) **	0.51 ± 0.08 (5)	0.47 ±0.10 (5) **
Y96F	−0.35 ± 0.72 (11) **	0.99 ± 0.03 (11)	0.74 ± 0.07 (10) **	−20.72 ± 2.12 (10) **	0.45 ± 0.03 (10)	0.25 ± 0.04 (10)
G97A	−3.51 ± 1.77 (12)	0.89 ± 0.06 (12)	0.90 ± 0.09 (10) **	−10.38 ± 4.38 (6) **	0.71 ± 0.13 (6)	0.66 ± 0.12 (6) **
	Selectivity filter – P2					
I200L	+1.33 ± 1.12 (5) **	1.06 ± 0.05 (5)	1.22 ± 0.14 (6) **	−25.37 ± 4.10 (5) **	0.38 ± 0.06 (5)	0.29 ± 0.07 (5)
I200V	−8.11 ± 1.26 (8)	0.73 ± 0.04 (8)	0.31 ± 0.02 (8)	−57.09 ± 4.00 (8) **	0.11 ± 0.02 (8)	0.06 ± 0.01 (8)
I200S	−5.37 ± 2.01 (5) **	0.82 ± 0.06 (5)	0.71 ± 0.09 (5) *	−15.06 ± 2.67 (5) **	0.56 ± 0.07 (5)	0.40 ±0.07 (5) *
I200T	−5.32 ± 2.02 (5)	0.82 ± 0.06 (5)	0.81 ± 0.18 (5) **	−10.12 ± 1.83 (5) **	0.67 ± 0.05 (5)	0.53 ± 0.09 (5) **
G201A	−0.20 ± 2.10 (5)	1.00 ± 0.08 (5)	0.80 ± 0.14 (5) **	−8.47 ± 2.64 (3) **	0.72 ± 0.07 (3)	0.46 ±0.03 (3) *
F202Y	−5.83 ± 1.86 (7)	0.81 ± 0.06 (7)	0.79 ± 0.16 (6) **	−20.20 ± 6.41 (4) **	0.49 ± 0.14 (4)	0.30 ±0.09 (4)
F202A	+0.93 ± 1.54 (8) **	1.05 ± 0.07 (8)	1.06 ± 0.11 (8) **	−4.49 ± 1.77 (8) **	0.85 ± 0.06 (8)	1.09 ±0.17 (8) **
F202M	−2.14 ± 0.90 (10)	0.92 ± 0.03 (10)	0.97 ± 0.09 (10) **	−10.94 ± 2.10 (5) **	0.65 ± 0.05 (5)	0.41 ±0.07 (5)

Europe PMC Funders Author Manuscripts

	Rb^+			Na^+		
	ΔE_{rev}	**P_{Rb}/P_K**	**I_{Rb}/I_K(−100mV)**	**ΔE_{rev}**	**P_{Na}/P_K**	**I_{Na}/I_K(−100mV)**
F202V	+1.22 ± 0.64 (5) **	1.05 ± 0.03 (5)	0.80 ± 0.13 (6) **	−6.29 ± 5.50 (5) **	0.85 ± 0.18 (5)	0.68 ±0.18 (5) *
F202L	−11.41 ± 1.89 (11)	0.65 ± 0.05 (11)	0.51 ± 0.07 (11)	−35.32 ± 4.29 (8) **	0.28 ± 0.07 (8)	0.22 ± 0.04 (8) **
G203A	−1.53 ± 1.63 (7)	0.95 ± 0.06 (7)	1.02 ± 0.08 (7) **	−8.38 ± 4.40 (6) **	0.78 ± 0.15 (6)	0.60 ± 0.10 (6) **
Pore helix – P1						
T89A	−2.36 ± 0.31 (14) **	0.91 ± 0.01 (14)	0.93 ± 0.07 (14) **	−28.04 ± 0.33 (5) **	0.33 ± 0.004 (5)	0.31 ± 0.02 (5) **
T89V	−7.89 ± 1.17 (13)	0.74 ± 0.03 (13)	0.70 ± 0.04 (13) **	−52.9 ± 10.89 (4) **	0.16 ± 0.06 (4)	0.13 ± 0.07 (4)
T89S	−2.74 ±0.68 (12) **	0.90 ± 0.02 (12)	0.91 ± 0.04 (12) **	−37.18 ± 0.97 (5) **	0.23 ± 0.01 (5)	0.30 ± 0.03 (5) **
V90L	−4.84 ± 0.72 (5)	0.83 ± 0.02 (5)	1.00 ± 0.03 (5) **	−59.06 ± 4.61 (5) **	0.10 ± 0.02 (5)	0.03 ± 0.01 (5)
V90S	−7.78 ± 1.18 (7)	0.74 ± 0.03 (7)	0.83 ± 0.08 (7) **	−26.83 ± 4.31 (6) **	0.36 ± 0.05 (6)	0.37 ± 0.07 (7) **
V90T	−6.70 ± 0.92 (9)	0.77 ± 0.03 (9)	1.07 ± 0.03 (9) **	−71.14 ± 3.82 (9) *	0.06 ± 0.01 (9)	0.06 ± 0.02 (9)
Outer pore mouth – P1 and P2						
A100T	−3.10 ± 1.97 (5)	0.89 ± 0.07 (5)	0.59 ± 0.03 (5) **	−47.82 ± 3.22 (5) **	0.15 ± 0.02 (5)	0.29 ± 0.04 (5) **
V206T	−5.35 ± 0.90 (8)	0.81 ± 0.03 (8)	0.70 ± 0.05 (8) **	−31.56 ± 2.84 (8) **	0.29 ± 0.03 (8)	0.15 ± 0.02 (8) **
A100T/V206T	−0.64 ± 0.52 (5) **	0.98 ± 0.02 (5)	0.95 ± 0.04 (5) **	−18.86 ± 3.48 (5) **	0.49 ± 0.07 (5)	0.42 ± 0.08 (5) **

The experimentally measured quantities were compared statistically using ANOVA

Mutants G95E, G95E/WT, Y96L, Y96M and Y96V were also examined but failed to generate functional channels.

* $P<0.05$

** $P<0.01$.

Table 2

Response to acidification of TASK-1 mutants

mutant	pK_a(−40)	acid sensitive current fraction	pK_a(+40)	acid sensitive current fraction
Wild type	6.66 ± 0.05 (13)	set to 1	6.57 ± 0.06 (13)	set to 1
Selectivity filter - P1				
I94S	7.34 ± 0.60 (3)	0.17 ± 0.08	7.48 ± 0.44 (4)	0.26 ± 0.08
I94T	7.62 ± 0.63 (4) *	0.47 ± 0.10	6.34 ± 0.53 (4)	0.23 ± 0.05
I94L	7.06 ± 0.12 (4)	1	6.83 ± 0.09 (4)	1
I94V	6.19 ± 0.21 (4)	1	6.18 ± 0.19 (4)	1
G95A	Assumed as WT	0.16 ± 0.07 (9)	Assumed as WT	0.23 ± 0.07 (9)
Y96F	8.48 ± 0.09 (8) **	0.77 ± 0.02	8.47 ± 0.07 (8) **	0.81 ± 0.03
G97A	7.60 ± 0.21 (5) **	0.67 ± 0.05	8.30 ± 0.21 (5) **	0.83 ± 0.04
Selectivity filter - P2				
I200S	Not fitted		6.86 ± 0.07 (3)	0.27 ± 0.04
I200T	7.54 ± 0.39 (5) **	0.86 ± 0.04	7.21 ± 0.53 (5)	0.62 ± 0.03
I200L	7.38 ± 0.15 (4)	0.77 ± 0.03	7.52 ± 0.09 (4) *	0.71 ± 0.04
I200V	6.50 ± 0.27 (5)	0.52 ± 0.02	7.35 ± 0.35 (6) *	0.58 ± 0.17
F202Y	7.73 ± 0.33 (4) **	0.18 ± 0.05	7.74 ± 0.55 (3) **	0.30 ± 0.03
Outer pore mouth – P1 and P2				
A100T	Assumed as WT	0.20 ± 0.08 (8)	Assumed as WT	0.17 ± 0.08 (8)
V206T	8.12 ± 0.13 (5) **	0.86 ± 0.02	8.25 ± 0.11 (5) **	0.88 ± 0.03
Pore helix – P1				
T89S	6.97 ± 0.08 (5)	0.89 ± 0.09	7.02 ± 0.15 (5)	0.83 ± 0.06
T89A	8.21 ± 0.09 (6) **	0.76 ± 0.04	8.19 ± 0.08 (6) **	0.79 ± 0.03
T89V	8.27 ± 0.16 (6) **	0.86 ± 0.04	8.46 ± 0.16 (6) **	0.86 ± 0.03
V90L	7.55 ± 0.07 (6) **	1	7.71 ± 0.09 (6) **	0.93 ± 0.02
V90T	7.18 ± 0.05 (4)	1	7.59 ± 0.16 (4) *	0.86 ± 0.01

The results are fitted to Eqn (2) of the text, that is to: $y = a.\left\{1 + \frac{[H^+]_o}{K_a}\right\}^{-1} + b$, where y is the fractional current. The acid sensitive fraction is computed as $a/(a + b)$. $pK_a = -\log_{10} K_a$. We have used ANOVA, with Dunnett's multiple comparisons test, to compare values for pK_a obtained from the best fit to the experimental results with those obtained for wild type.

Mutants shown in italics have $P_{Na}/P_K \leq 0.2$

* denotes significant differences with $P < 0.05$.

** denotes significant differences with $P < 0.01$.

Europe PMC Funders Author Manuscripts